Identification and PID Control for a Class of Delay Fractional-order Systems

Zhuoyun Nie, Qingguo Wang, Ruijuan Liu, and Yonghong Lan

***Abstract*—In this paper, a new model identification method is developed for a class of delay fractional-order system based on the process step response. Four characteristic functions are defined to characterize the features of the normalized fractional-order model. Based on the time scaling technology, two identification schemes are proposed for parameters' estimation. The scheme one utilizes three exact points on the step response of the process to calculate model parameters directly. The other scheme employs optimal searching method to adjust the fractional order for the best model identification. The proposed two identification schemes are both applicable to any stable complex process, such as higher-order, under-damped/over-damped, and minimum-phase/nonminimum-phase processes. Furthermore, an optimal PID tuning method is proposed for the delay fractional-order systems. The requirements on the stability margins and the negative feedback are cast as real part constraints (RPC) and imaginary part constraints (IPC). The constraints are implemented by trigonometric inequalities on the phase variable, and the optimal PID controller is obtained by the minimization of the integral of time absolute error (ITAE) index. Identification and control of a Titanium billet heating process is given for the illustration.**

***Index Terms*—Fractional-order system, time delay, identification, PID control, Titanium billet heating furnace.**

I. Introduction

FRACTIONAL order appears in many real dynamical processes naturally, such as heating furnace[1], flexible structures[2], materials with memory and hereditary effects[3], and a new electrical circuit element named "fractance"[4]. Compared with the integer model, fractional-order model often provides more reliable description for some real dynamical processes, especially when the Bode diagrams do not show slopes of integer multiplying of 20 dB/decade[5], or when the traditional integer models cannot fit the experiments data well. For these reasons, more and more attention has been paid to the problems of identification and control of fractional-order systems[6−9]. A recent survey of its development is presented in [10] and its applications are introduced in [11].

For unknown processes, fractional-order system identification becomes a difficult problem due to the fractional order present in the physical systems. The aim of identification of fractional-order system is to establish a fractional-order model to describe the system's physical behavior by the observed data. Since the model parameters in identifying consist now not only the coefficients but also the differentiation orders appearing nonlinearly, some standard tools, such as relay feedback method for integer models cannot be used directly to identify fractional-order systems if there is no fundamental improvement in the relay feedback theory. Therefore, the researches on the identification problem for fractional-order system have attracted lots of attention. An overview of the identification issue of fractional-order system is introduced in [12].

There have been some methods developed for the fractional-order system identification using continuous time models. In [13], linear least square (LS) optimization technique is used to estimate the coefficients of fractional differential equation, with the differentiation orders being fixed according to a prior knowledge. When the fractional differentiation orders are not available by the prior knowledge, output error methods are developed in [14], to provide estimation of both coefficients and differentiation orders by nonlinear optimization techniques instead of LS. The above two methods are based on classical identification methods whose parameters are estimated by minimizing a given criterion and data fitting. It is obvious that, the identification procedure becomes complicated when nonlinear optimization is involved[15]. Recently, an optimal identification algorithm is developed with a carefully selected initial value for a class of fractional order modeling[16].

Another identification approach has been presented for fractional-order systems in frequency domain. A new concept of continuous order-distribution is introduced through the development of a fractional/integer-order system identification, which allows the identification of both standard fractional/integer-order systems containing continuous or discrete terms as well as system with continuous order-distributions[17] . Recently, frequency response model identification for fractional-order systems is provided for the purpose of PID auto-tuning[18] . The model assumed to be fractional-order plus time delay form is obtained by model reduction from identified integer model. To estimate the time delay along with continuous-time fractional-order model, a linear filter is introduced for the model identification in an iterative manner by solving simple linear regression[19].

Manuscript received August 20, 2015; accepted February 18, 2016. This work was supported by National Natural Science Foundation of China (61403149, 61573298), Natural Science Foundation of Fujian Province (2015J01261, 2016J05165), and Foundation of Huaqiao University (Z14Y0002). Recommended by Associate Editor Antonio Visioli.

Citation: Zhuoyun Nie, Qingguo Wang, Ruijuan Liu, Yonghong Lan. Identification and PID control for a class of delay fractional-order systems. *IEEE/CAA Journal of Automatica Sinica*, 2016, **3**(4): 463−476

Zhuoyun Nie is with the School of Information Science and Engineering, Huaqiao University, Xiamen 361021, China (e-mail: yezhuyun2004@sina.com).

Qingguo Wang is with the Institute for Intelligent Systems, the University of Johannesburg, Johannesburg 2146, South Africa (e-mail: wangq@uj.ac.za).

Ruijuan Liu is with the School of Applied Mathematics, Xiamen University of Technology, Xiamen 361021, China (e-mail: liuruijuan0313@163.com).

Yonghong Lan is with the School of Information Engineering, Xiangtan University, Xiangtan 411105, China (e-mail: yhlan@xtu.edu.cn).

To obtain PID controller for a fractional-order process, Luo et al.[20] designed integer/fractional-order PID controller for a class of fractional-order system in terms of phase margin and the robustness against the loop gain variations. Based on the magnitude and phase measurements of the plant by relay feedback tests at a frequency of interest, Monje et al.[8−9] developed a method for the auto-tuning of fractional-order PID controllers. Combined with the frequency response estimation for a fractional-order system, an explicit PID tuning rule is proposed, which incorporates both the set-point tracking and the disturbance rejection case[18].

In this paper, a new model identification method is developed for a class of delay fractional-order model. The step responses of the normalized fractional-order model are used for the characteristic functions' definition and fitting. Combined with characteristic functions, the process is identified by time scaling technology. Two identification schemes are developed in the parameter estimation. The scheme one utilizes three exact points' data on the step response of the process to obtain the fractional-order model parameters. The other scheme employs single-variable optimization to adjust the fractional order for the proper parameters. The proposed two identification schemes are both applicable to any stable complex process, such as higher-order, under-damped/over-damped, and minimum-phase/nonminimum-phase processes. Furthermore, an optimal PID tuning method is proposed for the delay fractional-order model. The requirements on the stability margins and the negative feedback structure are cast as real part constraints (RPC) and imaginary part constraints (IPC). The constraints are implemented by trigonometric inequalities on the phase variable, and the optimal controller is obtained by solving a single-variable optimization problem to minimize the integral of time absolute error (ITAE) index. Application results on the Titanium billet heating furnace are provided for the illustration.

The remaining parts of this paper are organized as follows. In Section II, the proposed model identification method based on time scaling technology is developed. In Sections III, optimal PID controller tuning method is presented using ITAE rule. The simulation and comparison results in Section IV are given to illustrate the performance of the proposed methods. In Section V, application results on the titanium billet heating furnace are provided for model identification and control. Finally, conclusion is given in Section VI.

II. Process Model and Identification

In the real-world, many stable physical systems can be well characterized by fractional-order model with non integer-order derivatives. Suppose a stable process is modeled by a delay fractional-order system

$$G(s) = \frac{K}{Ts^{\alpha}+1}\mathrm{e}^{-Ls}, \tag{1}$$

where $L > 0$ is time delay, $T > 0$ is the time constant, K is the loop gain and $0 < \alpha < 2$ is the fractional order.

The step responses of (1) for different values of α with $K = 1$, $T = 0$ and $L = 0$ are given in Fig. 1, which shows that the fractional-order model in (1) provides rich complex dynamics, including oscillations and overshoot, to characterize any stable engineering process[9, 19]. It is obvious that, the fractional-order α dominates the behavior of the step response and results in significant performance difference for the case of $0 < \alpha \leq 1$ and $1 < \alpha < 2$. When $0 < \alpha \leq 1$, the outputs have no oscillation and tend to the reference signal very slowly; when $1 < \alpha < 2$, the oscillations occur in the outputs and are stranger when α is increasing. So, it motivates us to identify the process based on step response depending on the system parameters.

A. Time Scaling Analysis

The process model is normalized to be $K\tilde{G}(\tilde{s}) = G(s)$, where

$$\tilde{G}(\tilde{s}) = \frac{1}{\tilde{s}^{\alpha}+1}\mathrm{e}^{-\tau\tilde{s}}, \tag{2}$$

$\tilde{s} = \sqrt[\alpha]{T}s$ and $\tau = L/\sqrt[\alpha]{T}$. Denote the step responses by $y(t)$ for the system $G(s)$ and $\tilde{y}(\tilde{t}+\tau)$ for the normalized systems $\tilde{G}(\tilde{s})$. Note that, $\tilde{t}$ stands for the time coordinate in the case of $\tau = 0$, and the data $(\tilde{t}, \tilde{y}(\tilde{t}+0))$ will be collected and used in our identification.

According to definition of Laplace transform,

$$\mathcal{L}[f(t)] = F(s) = \int_0^{\infty} f(t)\mathrm{e}^{-st}\mathrm{d}t, \tag{3}$$

it is deduced that

$$\mathcal{L}\left[f(\frac{t}{a})\right] = aF(as), \quad a \in \mathbf{R}. \tag{4}$$

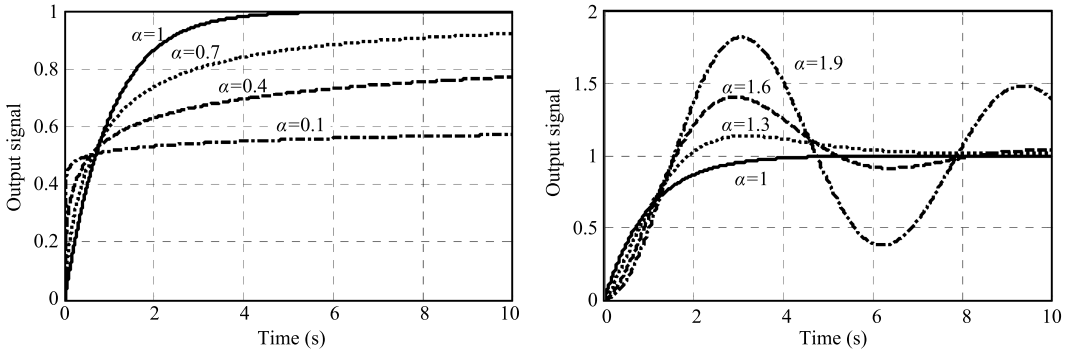

Fig. 1. The step responses for $0 < \alpha \leq 1$ and $1 < \alpha < 2$ with $K = 1$ and $T = 0$.

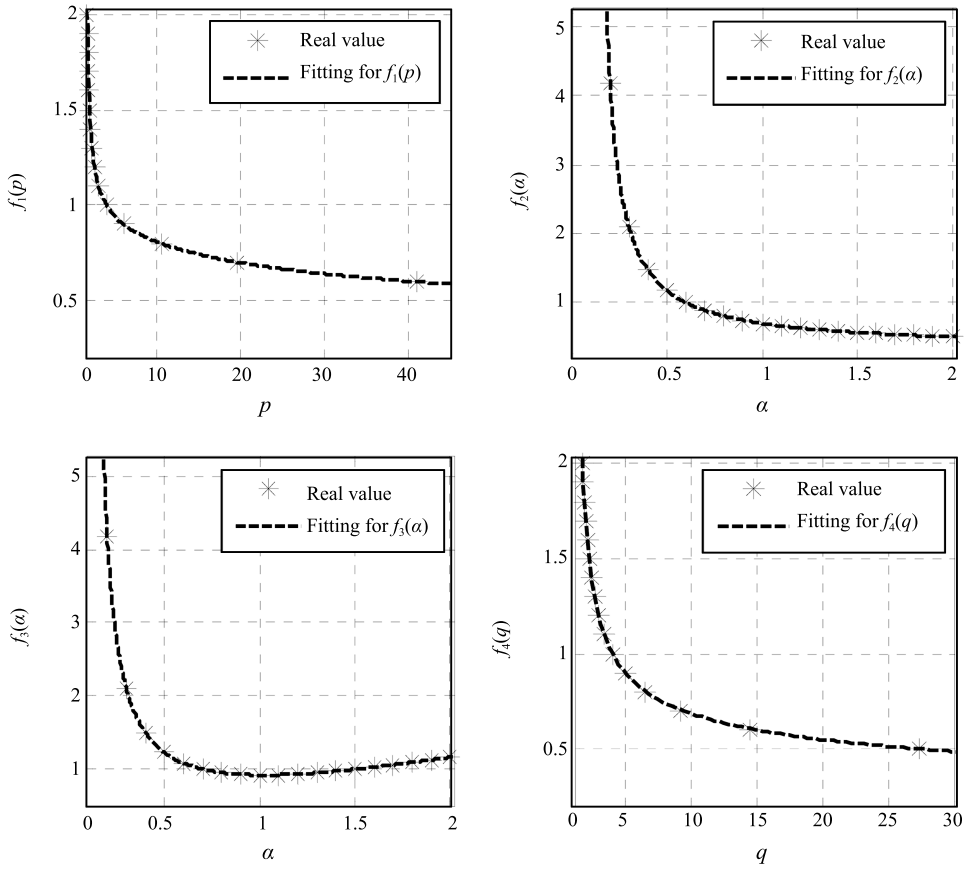

Fig. 2. Curve fitting for $f_1(p)$, $f_2(\alpha)$, $f_3(\alpha)$ and $f_4(q)$.

According to (4), when

$$y(t) = K\tilde{y}(\tilde{t}+\tau), \tag{5}$$

the following equation holds,

$$\tilde{t}+\tau = \frac{t}{\sqrt[\alpha]{T}}. \tag{6}$$

In this way, the relationship between $y(t)$ and $\tilde{y}(\tilde{t}+\tau)$ is well formulated by time scaling.

Denote the step response of the real process by $y_r(t)$. Since the process is modeled by (1), it is reasonable to assume $y_r(t) \approx y(t)$, and specify $y_r(t_i) = K\tilde{y}(\tilde{t}_i+\tau)$ at some points. Then, the parameters can be solved directly using (6). Here, two identifying schemes are proposed for the parameter estimation based on (6).

B. Identification by Three Points

The process gain K is obtained directly by

$$K = \frac{y_r(\infty)}{r(\infty)}, \tag{7}$$

for the stable process. Collect the responses data $(\tilde{t}, \tilde{y}(\tilde{t}+0))$ in Fig. 1, and choose $\tilde{y}(\tilde{t}_1) = \beta_1$, $\tilde{y}(\tilde{t}_2) = \beta_2$ and $\tilde{y}(\tilde{t}_3) = \beta_3$, where $\beta_1 < \beta_2 < \beta_3$ and $\tilde{t}_1 < \tilde{t}_2 < \tilde{t}_3$, in the rising up stage of the step response. Three points are specified as $y_r(t_1)/K = \beta_1$, $y_r(t_2)/K = \beta_2$ and $y_r(t_3)/K = \beta_3$, on the process responses, (6) gives the following equations:

$$\begin{cases} \tilde{t}_1+\tau = \dfrac{t_1}{\sqrt[\alpha]{T}}, \\ \tilde{t}_2+\tau = \dfrac{t_2}{\sqrt[\alpha]{T}}, \\ \tilde{t}_3+\tau = \dfrac{t_3}{\sqrt[\alpha]{T}}. \end{cases} \tag{8}$$

Before solving (8), four characteristic functions are defined

$$\begin{cases} f_1\left(\dfrac{\tilde{t}_3-\tilde{t}_1}{\tilde{t}_2-\tilde{t}_1}\right) := \alpha, \\ f_2(\alpha) := \tilde{t}_2 - \tilde{t}_1, \\ f_3(\alpha) := \tilde{t}_2, \\ f_4\left(\dfrac{\tilde{t}_2}{\tilde{t}_1}\right) := \alpha, \end{cases} \tag{9}$$

where

$$p := \frac{t_3-t_1}{t_2-t_1} = \frac{\tilde{t}_3-\tilde{t}_1}{\tilde{t}_2-\tilde{t}_1}, \tag{10}$$

$$q := \frac{t_2}{t_1} = \frac{\tilde{t}_2}{\tilde{t}_1}. \tag{11}$$

Then, the explicit solution of (8) is given by

$$\begin{cases} \alpha = f_1(p), \\ T = \left(\dfrac{t_2-t_1}{f_2(\alpha)}\right)^{\alpha}, \\ L = t_2 - f_3(\alpha)\sqrt[\alpha]{T}. \end{cases} \tag{12}$$

In (12), $\alpha > 0$ and $T > 0$ hold naturally, since $\tilde{t}_1 < \tilde{t}_2 < \tilde{t}_3$ and $t_1 < t_2 < t_3$. $L < 0$ would occur if

$$t_2 < \tilde{t}_2 \sqrt[\alpha]{T}, \tag{13}$$

because of the complex dynamics caused by high-order poles and zeros, actuator nonlinearities or time varying parameters. In this case, we set $L = 0$ and find the solutions of α and T using two points. Take $\tilde{y}(\tilde{t}_1) = \beta_1$, $\tilde{y}(\tilde{t}_2) = \beta_2$, and we have the solutions

$$\begin{cases} \alpha = f_4(q), \\ T = \left(\dfrac{t_2 - t_1}{f_2(\alpha)}\right)^{\alpha}, \\ L = 0. \end{cases} \tag{14}$$

In this paper, we set $\beta_1 = 0.2$, $\beta_2 = 0.6$ and $\beta_3 = 0.95$ which are listed in Table I as the recommended value for collection of data. Then, four characteristic functions are obtained by curve fitting, as shown in Fig. 2,

$$\begin{cases} f_1(p) = \dfrac{0.4053p^3 + 22.61p^2 + 14.85p - 41.29}{p^3 + 25.22p^2 - 4.519p - 44.52}, \\ f_2(\alpha) = \dfrac{0.3315\alpha + 0.2876}{\alpha - 0.1153}, \\ f_3(\alpha) = \dfrac{2.96\alpha^2 + 1.344\alpha + 4.814}{\alpha^3 - 5.488\alpha^2 + 16.21\alpha - 1.787}, \\ f_4(q) = \dfrac{0.2789q^2 + 14.85q + 11.26}{q^2 + 19.16q - 18.25}. \end{cases} \tag{15}$$

These four functions will play important roles in our process identification because the features of step responses of the normalized model (2) can be well characterized by them. Note that, for any different choice of β_i, the accuracy of the identification results only depend upon the fitting precision.

C. Optimal Identification

Theoretically, the model parameters can be calculated exactly if three points are specified on the step response by (12) or (14), but this would be a strict limitation on the whole curve matching for the responses. Recall that, the fractional-order α dominates the behavior or the shape of the step response. A good choice of α can guarantee a nice shape matching, which motivates us to develop an optimal identification scheme.

Take $\beta_1 = 0.4$ and $\beta_2 = 0.6$ as the recommended value to have $\tilde{y}(\tilde{t}_1) = \beta_1$ and $\tilde{y}(\tilde{t}_2) = \beta_2$, and the values of $\tilde{t}_1$ and $\tilde{t}_2$ are collected in Table II. The function $f_2(\alpha)$, as shown in Fig. 3, is updated in (15) by curve fitting

$$f_2(\alpha) = \frac{0.3704}{\alpha - 0.1097}. \tag{16}$$

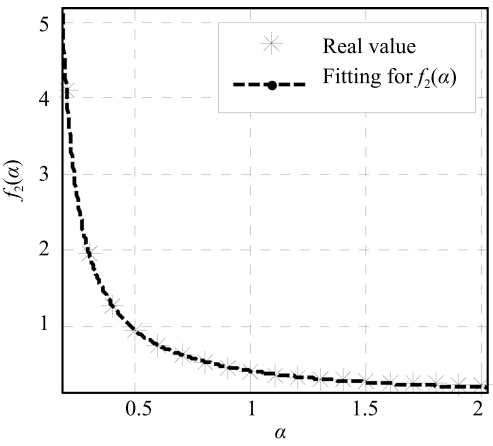

Fig. 3 Curve fitting for $f_2(\alpha)$.

TABLE I
$\tilde{t}_i$ FOR DIFFERENT α IN FIG. 1

α	$\tilde{t}_1$ $\beta_1 = 0.2$	$\tilde{t}_2$ $\beta_1 = 0.6$	$\tilde{t}_3$ $\beta_3 = 0.95$
0.1	$1/\infty$	31.92	∞
0.2	$1/\infty$	4.180	∞
0.3	0.0064	2.102	> 8000
0.4	0.0214	1.497	> 600
0.5	0.0448	1.228	126.3
0.6	0.0744	1.083	41.41
0.7	0.1082	0.9983	17.55
0.8	0.1449	0.952	8.61
0.9	0.1834	0.927	4.71
1.0	0.2233	0.9164	3.02
1.1	0.264	0.9188	2.265
1.2	0.3052	0.9297	1.911
1.3	0.3470	0.9470	1.72
1.4	0.3890	0.9693	1.612
1.5	0.4312	0.9954	1.55
1.6	0.4736	1.0244	1.517
1.7	0.5160	1.0557	1.501
1.8	0.5585	1.0888	1.50
1.9	0.6010	1.1236	1.507
2.0	0.6436	1.1594	1.521

TABLE II
$\tilde{t}_i$ FOR DIFFERENT α IN FIG. 2

α	$\tilde{t}_1$ $\beta_1 = 0.4$	$\tilde{t}_2$ $\beta_1 = 0.6$
0.1	0.0099	31.92
0.2	0.0771	4.180
0.3	0.1551	2.102
0.4	0.2236	1.497
0.5	0.2824	1.228
0.6	0.3342	1.083
0.7	0.3816	0.9983
0.8	0.4262	0.952
0.9	0.4690	0.927
1.0	0.5110	0.9164
1.1	0.5524	0.9188
1.2	0.5937	0.9297
1.3	0.6350	0.9470
1.4	0.6764	0.9693
1.5	0.7180	0.9954
1.6	0.7596	1.0244
1.7	0.8014	1.0557
1.8	0.8433	1.0888
1.9	0.8853	1.1236
2.0	0.9274	1.1594

In our optimal identification, integral square error (ISE) between $y(t)$ and $y_r(t)$ is introduced to find the optimal solution. Then, the minimization problem can be formulated by

$$J_{id} = \min_{\alpha} \left[\int_0^{t*} |y(t) - y_r(t)|^2 \mathrm{d}t \right], \tag{17}$$

$$\text{s.t.} \begin{cases} T = \left(\dfrac{t_2 - t_1}{f_2(\alpha)} \right)^{\alpha}, \\ L = \max \left(t_2 - f_3(\alpha) \sqrt[\alpha]{T}, \quad 0 \right), \end{cases} \tag{18}$$

and solved easily by MATLAB function "fminbnd".

D. Algorithms

The proposed two identification schemes are summarized by the following algorithms.

Algorithm 1. Three points identification (Model 1)

Step 1. Set the recommended value $\beta_1 = 0.2$, $\beta_2 = 0.6$ and $\beta_3 = 0.95$, and calculate the process gain K by (7).

Step 2. Collect t_1, t_2 and t_3 from the step response of the real process to have $y_r(t_1)/K = \beta_1$, $y_r(t_2)/K = \beta_2$ and $y_r(t_3)/K = \beta_3$.

Step 3. Calculate p, q by (10) and (11), respectively.

Step 4. Calculate the value of four functions in (15) to have $\alpha = f_1(p)$, $\tilde{t}_2 - \tilde{t}_1 = f_2(\alpha)$, $\tilde{t}_2 = f_3(\alpha)$ and $\alpha = f_4(q)$.

Step 5. If $t_2 > \tilde{t}_2 \sqrt[\alpha]{T}$, determine the parameters α, T and L by (12), otherwise, by (14).

Algorithm 2. Optimal identification (Model 2)

Step 1. Set the recommended value $\beta_1 = 0.4$ and $\beta_2 = 0.6$, and calculate the process gain K by (7).

Step 2. Collect t_1 and t_2 from the step response of the real process to have $y_r(t_1)/K = \beta_1$ and $y_r(t_2)/K = \beta_2$.

Step 3. Set an initial value of $\alpha = \alpha^* \in (0, 2)$.

Step 4. Update $f_2(\alpha)$ by (16), and calculate T and L by (18).

Step 5. Calculate the cost function (17). If convergent, stop; otherwise, set a new value $\alpha = \alpha_i$ by "fminbnd", and go to Step 4.

In (15) and (16), to reduce the fitting error, rational functions are used with proper order, for curve fitting, which confirms the accuracy of the identification results. Obviously, Algorithm 1 provides a fast identification with only three points used in the calculation, while Algorithm 2 provides more accurate identification results by optimal searching.

Remark 1. The proposed identification procedures in Algorithm 1 and Algorithm 2 allow long dead time, large phase lag and unstable zeros of the system are due to the introduced time delay in the fractional-order model. They can be successfully approximated with equivalent time delay[18].

Remark 2. The proposed identification method is applicable to a wide range of engineering processes. If the process is unstable, one can stabilize the process first by a proportional controller. Then, the method becomes applicable.

Remark 3. The measured noise or disturbance is inevitable in the real process and brings identification errors. To guarantee the accuracy, a filtering algorithm, such as median filtering, can be employed to make pretreatment of the measured data. Then, the measured noise or disturbance is limited.

Remark 4. A similar identification method can be found in [16] for the same model (1). Based on the step response, optimal fitting is carried out with carefully selected initial parameters. For the same points, both methods in this paper and in [16], are trying to extract some typical features of the step response for the model identification. Rather than the direct optimal computation, our basic idea is to make time scaling analysis for the process model (1) and its normalized model (2). Based on such time scaling relationship, the proposed two identification schemes are developed under a unified framework. Then, solving equation set by three exact points or by optimal response shape matching with two points is logical.

E. Simulation Study

To illustrate the utility of the proposed identification method, four typical processes, including minimum phase processes and nonminimum phase processes, are discussed in the simulations.

Process 1. Over-damped process with zero and time delay

$$G_{p1} = \frac{2s+1}{(s+1)^3} \mathrm{e}^{-0.5s}. \tag{19}$$

Process 2. Under-damped process with zero and time delay

$$G_{p2} = \frac{4s+1}{(9s^2+3s+1)(s+1)} \mathrm{e}^{-0.5s}. \tag{20}$$

Process 3. Over-damped process with positive zero and time delay

$$G_{p3} = \frac{-3s+1}{(s+1)^3} \mathrm{e}^{-s}. \tag{21}$$

Process 4. Under-damped process with positive zero and time delay

$$G_{p4} = \frac{-5s+1}{(9s^2+3s+1)(s+1)} \mathrm{e}^{-6s}. \tag{22}$$

The simulations are carried out for the case when the high-order models G_{p1}-G_{p4} have already known to provide the step response data. The identification procedures can also be viewed as model reduction for high-order processes. The above processes are identified to be fractional-order plus time delay models in (1) and a zero initial condition is assumed. The model performance will be compared with a frequency identification method[18].

The basic idea behind the frequency method[18] is to specify a point on the frequency response

$$G_p(\mathrm{j}\omega) = G(\mathrm{j}\omega), \tag{23}$$

which gives the amplitude condition and phase condition to solve T and L for a given value ofα. The parameters are finally determined by solving a single-variable optimization problem to minimize the norm of the frequency response errors between the process and the fractional model:

$$\min_{\alpha}\left[\sum_{i=1}^{n}\left|G_p(\mathrm{j}\omega_i)-G(\mathrm{j}\omega_i,\alpha)\right|^2\right],$$
$$0\le\omega 1<\omega 2<\cdots<\omega u,$$
$$\begin{cases}k=G_p(0),\\ T=\tau^{\alpha},\\ L=\dfrac{-\angle G_p(\mathrm{j}\omega)+\arctan 2(\tilde{A},\tilde{B})}{\omega},\end{cases}\tag{24}$$

where

$$\begin{cases}\tau=\left(\dfrac{-\cos(\frac{\alpha\pi}{2})|G_P(\mathrm{j}\omega)|^2\omega^{\alpha}+\sqrt{A+B}}{|G_P(\mathrm{j}\omega)|^2\omega^{2\alpha}}\right)^{\frac{1}{\alpha}}\\ A=\cos^2\left(\dfrac{\alpha\pi}{2}\right)|G_p(\mathrm{j}\omega)|^4\omega^{2\alpha}\\ B=|G_p(\mathrm{j}\omega)|^2\omega^{2\alpha}(k^2-|G_p(\mathrm{j}\omega)|^2)\\ \tilde{A}=-\sin\left(\dfrac{\alpha\pi}{2}\right)\tau^{\alpha}\omega^{\alpha}\\ \tilde{B}=\cos\left(\dfrac{\alpha\pi}{2}\right)\tau^{\alpha}\omega^{\alpha}+1\\ \omega\approx\omega_u\ (\text{the ultimate frequency of } G_P)\end{cases}$$

The identification results are given in Table III, and the performance in step responses and frequency responses are given in Figs. 4 and 5. It shows that the proposed method successfully estimates the fractional-order model by step response for all the investigated process with fairly good accuracy. Compared with the frequency method[18], the proposed optimal identification model provides better step response fitting to the real process.

Regarding the frequency response, the proposed models can also fit the processes well. The main fitting error for the nonminimum phase process is caused by the right plane zero, which is equivalent to time delay in the fractional-order model. In the proposed method, such equivalent treatment does not affect the fitting accuracy of the portion of minimum phase. One can see that, when undershoot is ending in Fig. 4, the proposed models follow the step responses of G_{p3} and G_{p4} with little error. So, it is obvious that, there is a trade-off between the step response fitting and frequency response fitting.

III. PID TUNING

In this section, a PID controller tuning method is developed for delay fractional-order processes. The proposed PID tuning rule is derived by ITAE minimization with the constraints on the stability margins.

Since the open loop gain of the Process 1 is less than unity over high frequency range and will not affect stability, the paper measures the robustness by the gain margin A and phase margin ϕ,

$$1+AG(\mathrm{j}\omega_p)C(\mathrm{j}\omega_p)=0,\tag{25}$$

$$1+\mathrm{e}^{-\mathrm{j}\phi}G(\mathrm{j}\omega_g)C(\mathrm{j}\omega_g)=0,\tag{26}$$

where ω_p and ω_g are the phase and gain crossover frequencies of the loop, respectively. According to [21−22], these two

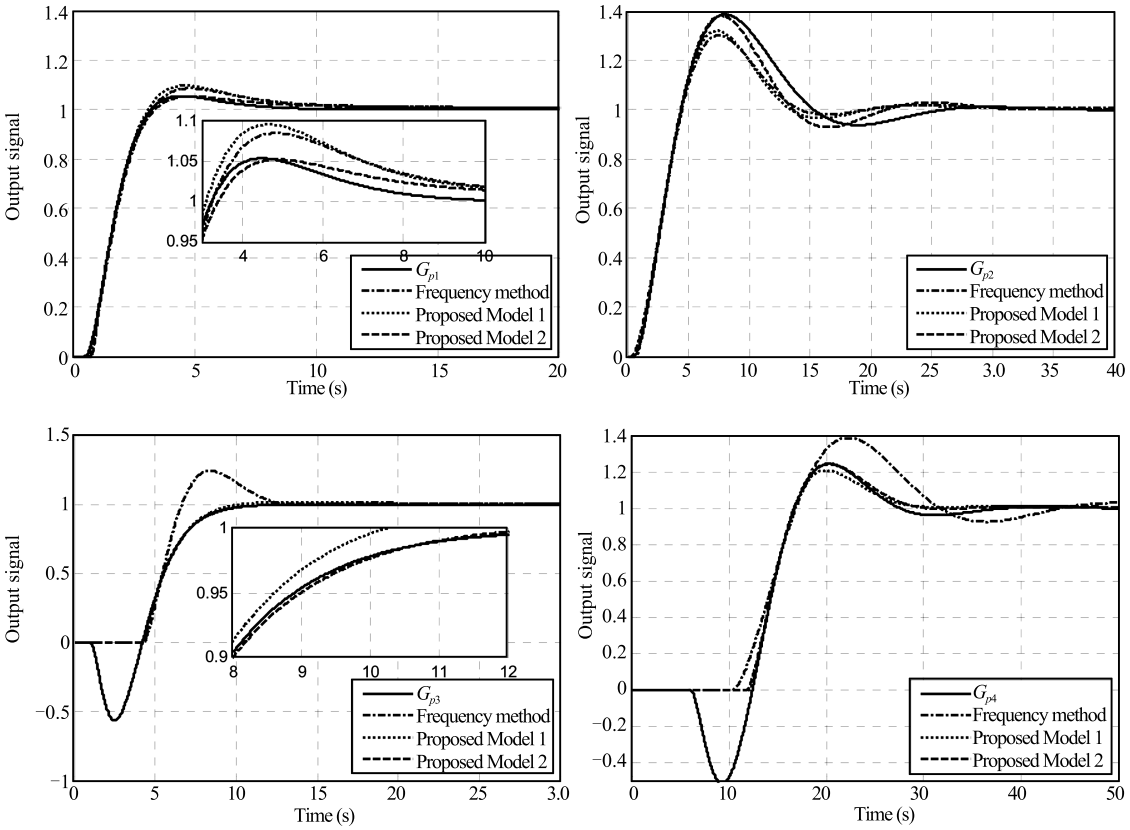

Fig. 4. Results of the process identification method.

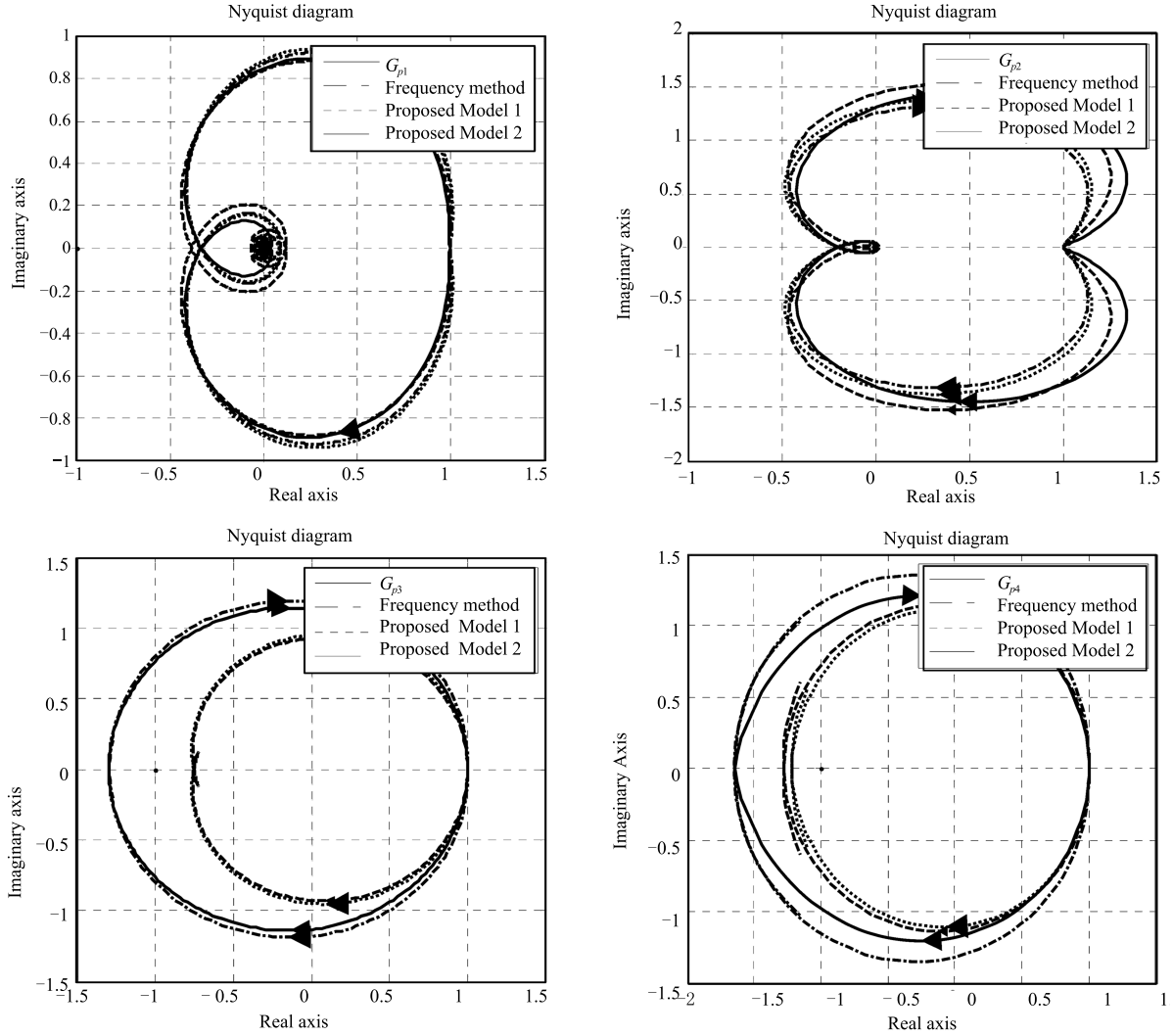

Fig. 5. Frequency responses.

TABLE III
IDENTIFICATION RESULTS FOR FOUR ILLUSTRATIVE EXAMPLES

Process	Proposed (Model 1)	J_{id}	Proposed (Model 2)	J_{id}	Frequency fitting in [18]	J_{id}
1	$\frac{1}{1.2229s^{1.2417}+1}\mathrm{e}^{-0.6786s}$	0.8508	$\frac{1}{1.0905s^{1.16}+1}\mathrm{e}^{-0.783s}$	0.2887	$\frac{1}{1.2427s^{1.2226}+1}\mathrm{e}^{-0.7158s}$	0.7579
2	$\frac{1}{3.5294s^{1.5216}+1}\mathrm{e}^{-0.6265s}$	10.5945	$\frac{1}{4.2556s^{1.58}+1}\mathrm{e}^{-0.37336s}$	5.0937	$\frac{1.0033}{3.5277s^{1.4973}+1}\mathrm{e}^{-0.6699s}$	10.0240
3	$\frac{1}{1.8726s^{1.0694}+1}\mathrm{e}^{-4.2191s}$	46.8204	$\frac{1}{1.6631s^{1.02}+1}\mathrm{e}^{-4.3594s}$	46.5919	$\frac{1.0002}{1.5932s^{1.4409}+1}\mathrm{e}^{-4.2965s}$	80.1147
4	$\frac{1}{3.8241s^{1.3969}+1}\mathrm{e}^{-12.1103s}$	81.148	$\frac{1}{4.4894s^{1.44}+1}\mathrm{e}^{-11.8618s}$	80.6847	$\frac{1}{9.1595s^{1.5844}+1}\mathrm{e}^{-10.385s}$	129.5714

crossover frequencies satisfy $\omega_p \approx A\omega_g$, which motivates us to introduce an additional parameter γ in the formulation

$$\omega_p = \gamma\omega_g, \quad \gamma > 1. \tag{27}$$

This parameter γ plays the same role as ω_p, but it will provide convenience in the analysis of (25) and (26) uniformly under the same frequency variable ω_g.

The constraints on the stability margins are formulated by $A \geq A^*$ and $\pi \geq \phi > \phi^*$, where A^* and ϕ^* are stability lower bounds, and they are determined by the maximum closed-loop amplitude ratio M_T[23],

$$A^* = 1 + \frac{1}{M_T}, \quad \phi^* = 2\sin^{-1}\left(\frac{1}{2M_T}\right). \tag{28}$$

On the other hand, we also require the negative feedback control

$$u(t) = k_p e(t) + k_i \int_0^\infty e(t)\mathrm{d}t + k_d \mathrm{d}e(t), \tag{29}$$

with positive controller parameters $k_p > 0$, $k_i \geq 0$ and $k_d \geq 0$.

The transient performance is measured by ITAE index of the step response, that is

$$J_{\rm ITAE} = \int_0^\infty t\,|e(t)|{\rm d}t, \tag{30}$$

where $e(t) = r(t) - y(t)$ is the error signal. Combined with all the constraints, the controller design problem is formulated by

$$\min_{k_p,k_i,k_d} J_{\rm ITAE} = \int_0^\infty t\,|e(t)|{\rm d}t,$$
$$\text{s.t.} \quad \begin{cases} A \geq A^*, \\ \pi \geq \phi > \phi^*, \\ k_p > 0, \\ k_i \geq 0, \\ k_d \geq 0. \end{cases} \tag{31}$$

The problem in (31) can be solved by some classical global searching methods or by intelligent algorithms, such as particle swarm optimization (PSO) or genetic algorithm (GA), without theoretical analysis. In this paper, we try to investigate the constraints (31) and develop an implemented searching algorithm to solve this problem. The constraints in (31) will be analyzed and converted to the implemented form: real parts constraints (RPC) and imaginary parts constraints (IPC), with the help of two characteristic equations (25) and (26).

A. RPC

Let us consider the real parts of (25) and (26), which lead to

$$k_p = {\rm Re}\left[-\frac{1}{AG({\rm j}\gamma\omega_g)}\right] = \frac{a}{A(a^2+b^2)}, \tag{32}$$

$$k_p = {\rm Re}\left[-\frac{\exp({\rm j}\phi)}{G({\rm j}\omega_g)}\right] = \frac{c\cos\phi + d\sin\phi}{(c^2+d^2)}, \tag{33}$$

where

$$a = {\rm Re}(-G({\rm j}\gamma\omega_g)),\ \ b = {\rm Im}(-G({\rm j}\gamma\omega_g)),$$
$$c = {\rm Re}(-G({\rm j}\omega_g)),\quad\ \ d = {\rm Im}(-G({\rm j}\omega_g)).$$

The relationship of gain margin and phase margin is derived by the following equation

$$A = \frac{a\sqrt{c^2+d^2}}{\sin(\phi+\alpha)(a^2+b^2)}, \tag{34}$$

where

$$\alpha = \begin{cases} \arctan\left(\dfrac{c}{d}\right), & c>0,\ d>0, \\ \pi - \arctan\left(\dfrac{c}{|d|}\right), & c>0,\ d<0, \\ -\pi + \arctan\left(\dfrac{|c|}{|d|}\right), & c<0,\ d<0, \\ -\arctan\left(\dfrac{|c|}{d}\right), & c<0,\ d>0. \end{cases} \tag{35}$$

Therefore, the constraints $k_p > 0$, and $A \geq A^*$, are equivalent to the following inequalities

$$RPC: \begin{cases} 0 < \sin(\phi+\alpha) \leq \dfrac{a\sqrt{c^2+d^2}}{A^*(a^2+b^2)}, & a>0, \\ \phi^* \leq \phi < \pi. \end{cases} \tag{36}$$

B. IPC

The imaginary parts of (25) and (26) are given by

$$k_d\gamma\omega_g - \frac{k_i}{\gamma\omega_g} = {\rm Im}\left[-\frac{1}{AG({\rm j}\gamma\omega_g)}\right] = \frac{-b}{A(a^2+b^2)}, \tag{37}$$

$$k_d\omega_g - \frac{k_i}{\omega_g} = {\rm Im}\left[-\frac{\exp({\rm j}\phi)}{G({\rm j}\omega_g)}\right] = \frac{c\sin\phi - d\cos\phi}{(c^2+d^2)}, \tag{38}$$

which are solved to get

$$\begin{cases} k_i = -\dfrac{b\gamma\omega_g\sin(\phi+\alpha) - a\omega_g\gamma^2\cos(\phi+\alpha)}{a\sqrt{c^2+d^2}\,(\gamma^2-1)}, \\ k_d = -\dfrac{b\gamma\sin(\phi+\alpha) - a\cos(\phi+\alpha)}{a\omega_g\sqrt{c^2+d^2}\,(\gamma^2-1)}. \end{cases} \tag{39}$$

Then, the constraints $k_d \geq 0$ and $k_i \geq 0$ are converted to

$$IPC: \max\left(\frac{b\gamma}{a}, \frac{b}{a\gamma}\right) \leq \frac{1}{\tan(\phi+\alpha)}. \tag{40}$$

C. Implementing Optimal Tuning

Based on the analysis above, an explicit PID controller tuning rule and the achieved gain margin are given by

$$\begin{cases} k_p = \dfrac{a}{A(a^2+b^2)} = \dfrac{1}{\sqrt{c^2+d^2}}\sin(\phi+\alpha), \\ k_i = -\dfrac{b\gamma\omega_g\sin(\phi+\alpha) - a\omega_g\gamma^2\cos(\phi+\alpha)}{a\sqrt{c^2+d^2}\,(\gamma^2-1)}, \\ k_d = -\dfrac{b\gamma\sin(\phi+\alpha) - a\cos(\phi+\alpha)}{a\omega_g\sqrt{c^2+d^2}\,(\gamma^2-1)}, \\ A = \dfrac{a\sqrt{c^2+d^2}}{\sin(\phi+\alpha)(a^2+b^2)}. \end{cases} \tag{41}$$

Theoretically, a suitable value of (ϕ, ω_g, γ) determines a robust stabilizing PID controller and the achieved gain margin in (41). For example, for some typical performance specifications on gain margin A_o, phase margin ϕ_o and the closed-loop bandwidth ω_B, we can set $(\phi, \omega_g, \gamma) \approx (\phi_o, \omega_B, A_o)$ as a recommended value for a robust PID controller in (41) or as an initial value for the optimal searching.

Remark 5. In [21−24], (ϕ, ω_g, A), (ϕ, ω_p, A) or $(\phi, \omega_g, \omega_p, A)$ are used to calculate PID controller parameters, involving some complex computation to solve (25) and (26), the two coupled nonlinear equations. In this paper, with basic variables (ϕ, ω_g, γ), the gain margin and three controller parameters are all decoupled from each other in (41). An explicit PID controller will be more applicable in the practical engineering, which is one of the advantages of the proposed tuning method.

Since (36) and (40) are formulated as trigonometric inequalities on ϕ, RPC and IPC are solved to be

$$\underline{\phi}(\omega_g, \gamma) < \phi < \overline{\phi}(\omega_g, \gamma), \tag{42}$$

where $\overline{\phi}(\omega_g,\gamma)$ and $\underline{\phi}(\omega_g,\gamma)$ stand for the upper bound and lower bound, respectively. Obviously, these two bounds are dependent on an admissible (ω_g,γ). In this way, (42) gives an exact parameter's range, and will help us to find an admissible region of (ϕ,ω_g,γ), which provides great convenience for the optimal searching.

With the equivalent constraint in (42), the optimal controller design problem in (39) can be rewritten in the implemented form

$$\begin{aligned}&\min J_{\mathrm{ITAE}}=\int_0^\infty t\,|e(t)|\mathrm{d}t,\\&\text{s.t.}\quad \underline{\phi}(\omega_g,\gamma)<\phi<\overline{\phi}(\omega_g,\gamma).\end{aligned}\tag{43}$$

This problem can be solved by MATLAB function "fminbnd" in three dimensions. Set the initial value of (ω_g,γ), and carry on the single-variable searching on ϕ within $[\underline{\phi}(\omega_g,\gamma),\overline{\phi}(\omega_g,\gamma)]$. The value of (ω_g,γ) will be updated by "fminbnd" for the iterations. When finishing the optimal searching in three dimensions, the optimal robust PID controller is decided by (41) accordingly as well as the achieved gain margin, phase margins and two crossover frequencies.

The proposed tuning scheme is summarized by the following algorithm.

Algorithm 3. Optimal PID tuning

Step 1. Give the specification of M_T and calculate the lower bounds of stability margins A^* and ϕ^*.

Step 2. Set the initial value of (ω_g,γ).

Step 3. Solve RPC and IPC by trigonometric calculations to obtain $[\underline{\phi}(\omega_g,\gamma),\overline{\phi}(\omega_g,\gamma)]$.

Step 4. Carry on single-variable searching on ϕ within $[\underline{\phi}(\omega_g,\gamma),\overline{\phi}(\omega_g,\gamma)]$ by "fminbnd".

Step 5. If convergent, go to Step 6; otherwise, update the value of (ω_g,γ) by "fminbnd", and go to Step 3.

Step 6. Substitute the resultant value of (ϕ,ω_g,γ) into (41) for the optimal PID controller.

D. Continuing Simulation Study

Regarding the optimal identified Model 2 in Table III, PID controllers are designed by the proposed method for different values of M_T. Tuning results are exhibited in Table IV, which show that, the maximum closed-loop amplitude ratio M_T is proportional to the overshoot in most cases. With a suitable value of M_T specified, the overshoot will be avoided or limited in the step response.

To illustrate the tuning algorithm, PID controller tuning for the Model 2 of the Process 1 is considered. In Step 1, set $M_T=1$, and calculate the lower bounds of the stability margins, $A^*=2$ and $\phi^*=\pi/3$. Given the initial value of $(\omega_g,\gamma)=(0.8,3)$ in Step 2, RPC and IPC are obtained in Step 3:

$$\begin{cases}0<\sin(\phi+0.1436)\le 1.2568,\\ \dfrac{\pi}{3}\le\phi<\pi,\\ -0.0754\le\dfrac{1}{\tan(\phi+0.1436)},\end{cases}\tag{44}$$

$$1.0472<\phi\le 1.4272.\tag{45}$$

TABLE IV
PROPOSED PID PARAMETERS FOR THE IDENTIFIED MODEL 2

Process	M_T	k_p	k_i	k_d	Overshoot (%)
1	1	1.2893	0.7587	0.5747	3.3
	1.2	1.2624	0.7361	0.5885	2.6
	1.4	1.2551	0.7653	0.6021	4.2
2	1	4.7749	0.9562	4.6739	11.1
	1.2	6.2443	1.2211	4.3948	14.9
	1.4	6.8523	1.505	4.0934	21.1
3	1	0.266	0.1071	0.3569	0.2
	1.2	0.5505	0.1579	0.6441	3.2
	1.4	0.5510	0.1582	0.6550	3.2
4	1	0.3010	0.0583	0.9809	4.49
	1.2	0.3074	0.0580	0.9874	6.87
	1.4	0.3157	0.0581	0.9985	7.4

In Step 4, single-variable searching is carried on in the phase range (45) to obtain the minimized index $J_{\mathrm{ITAE}}=2.6694$. Update the value of (ω_g,γ) for the further searching. Finally, three variables (ϕ,ω_g,γ) are found convergent to $(1.2786,\ 0.2965,\ 3.2687)$, and the optimal PID controller is determined by (41),

$$C(s)=1.2893+\frac{0.7587}{s}+0.5747s.\tag{46}$$

Simultaneously, the achieved control performances are obtained

$$A=2.05\,(\omega_g=0.3),\ \phi=1.27\,(\omega_p=0.96),\ J_{\mathrm{ITAE}}=1.74.\tag{47}$$

A comparison is made with the design method in [18], which is also using ITAE tuning rule but with no limitation on the stability margin. In [18], the controller parameters are given in Table V, which are obtained based on the frequency fitting model in Table III. In the comparison, we set the controller parameters in Table IV with $M_T=1$.

TABLE V
CONTROLLER PARAMETERS IN [18]

Process	k_p	k_i	k_d
1	1.3447	1.0022	0.6215
2	2.3722	1.1933	4.7102
3	0.3477	0.1731	0.5272
4	0.2624	0.0645	1.3623

Step response and load disturbance rejection are considered in Fig. 6. Table VI presents ITAE value, overshoot, and the achieved gain and phase margins of the resultant systems. From the tuning results, one can find that the proposed method achieves lower ITAE value and smaller overshoot than results of [18]. Two reasons can support this result: 1) accurate identified models allow better tuning performance for model-based tuning rules. 2) with the limitation on the maximum closed-loop amplitude ratio M_T, ITAE tuning rule would be more applicable in the practical application.

TABLE VI
TUNING RESULTS AND COMPARISON

Process	Proposed PID parameters (Proposed Model 2)				PID parameters[18] (Frequency fitting model)			
	ITAE	Overshoot (%)	Gain margin	Phase margin	ITAE	Overshoot (%)	Gain margin	Phase margin
1	199.11	5	2.907	70.5	199.6429	17	2.7797	61.2
2	236.72	11.9	1.5399	32.3	302.9330	30	1.7298	53.1
3	1.2462E+03	1.8	2.8741	62.4	1.2614E+03	31	2.2029	42
4	1.1269E+04	20.8	2.0114	56.3	1.1303E+04	24.5	1.7681	50.4

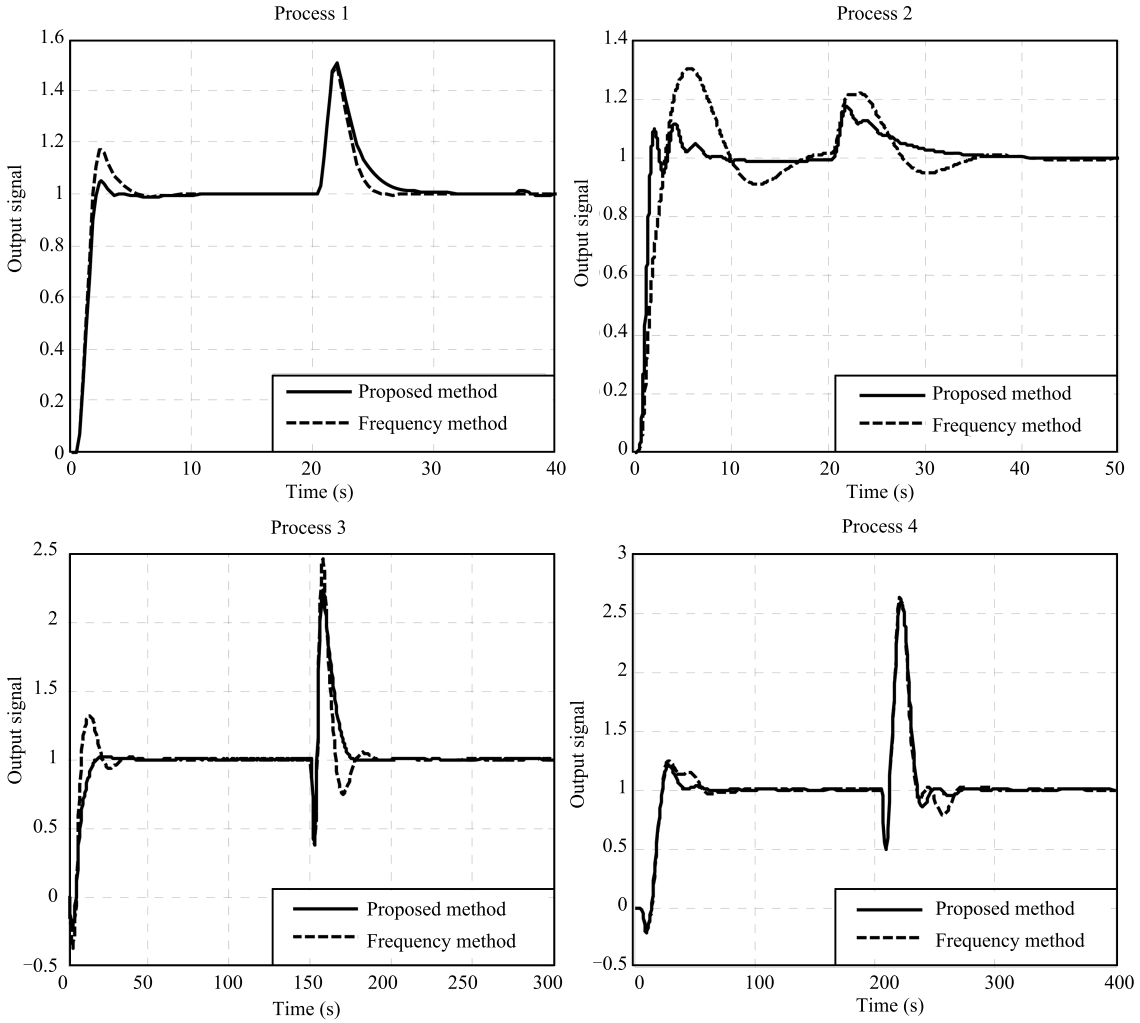

Fig. 6. Closed-loop responses of the PID control systems.

IV. Application to Titanium Billet Heating Furnace

Fractional-order dynamics appears naturally in the heating process when heat conduction occurs between the operating variable (input signal) and the measured physical variable (output signal). An example of heating furnace was considered in [25], which shows that the fractional-order model gives more exact description of the heating process than integer-order model.

Let us consider the temperature control problem of the titanium billet furnace[26]. The titanium billet furnace is divided into three heating areas and the temperature is controlled separately for each area (see Fig. 7). Two kinds of burners, including twelve 200 kW burners and six 350 kW burners, are used in parallel for different heating schedules. The mixed natural gas and air are burned through the 18 burners distributed on both sides of the furnace symmetrically.

The temperature control system is depicted in Fig. 8. Each burner is controlled by a pulse-controller PSF778L independently. The pulse-controller for each burner provides a precise control for the ratio of air and gas, and greatly improves the heating efficiency. All the burners work under the heating task assignment of burners' auto-setting controller PFA700 according to the total control actions generated by the controller SE-504, which is implemented in the form of PID. Note that, PFA700 also controls the process as an inner feedback

control loop to guarantee the basic dynamic performance of the heating process. The temperature feedback signals are measured by 6 thermocouples distributed in three areas.

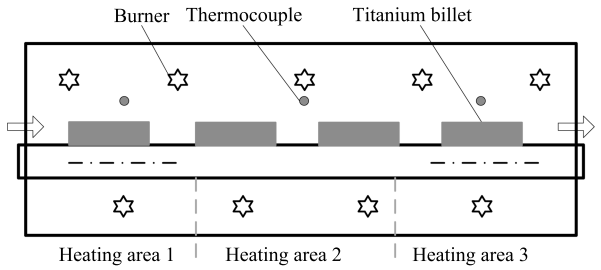

Fig. 7. Titanium billet heating furnace.

Now, consider the model identification for the heating process. We obtain the measured data from a real Titanium billet heating furnace in the first heating stage, with the target temperature 850 °C, which can be viewed as the step response of the heating process. All the measured data are plotted in Fig. 9. It is obvious that, the measured noise is inevitably involved in the sampled data. Especially, the temperature jumping occurs during the whole response, which is caused by the pulse flame of the burners near the thermocouples. To attenuate such temperature jumping and noise, median filtering method is employed to deal with the measured temperature value. Fig. 10 shows the median filtering results. The identification procedure for the Heating area 1 is presented to give the illustration. In the inner control loop, the heating process achieves the setting temperature slowly, that is $y(\infty) \approx 850\,^{\circ}\mathrm{C}$. The process gain is approximately to be $K \approx 1$.

The process is firstly identified by three points method. Collect $t_1 = 20\,\mathrm{min}$, $t_2 = 81\,\mathrm{min}$ and $t_3 = 374\,\mathrm{min}$ by Step 2 in Algorithm 1. The process is identified by (21),

$$\frac{1}{55.078s^{0.909}+1}\mathrm{e}^{-4.91s}. \tag{48}$$

Then, optimal identification is carried on by Algorithm 2. The cost function (26) is depicted in Fig. 11, and the optimal fractional-order is found by single-variable searching. The process is identified to be

$$\frac{1}{67.1867s^{0.94}+1}\mathrm{e}^{-5.21s}. \tag{49}$$

It is obvious that the step responses of the two resultant models, given in Fig. 12, are very close to the response of the real heating process. In the frequency domain, one can estimate frequency response with fixed frequency resolution using spectral analysis in Fig. 13. It can be seen that the

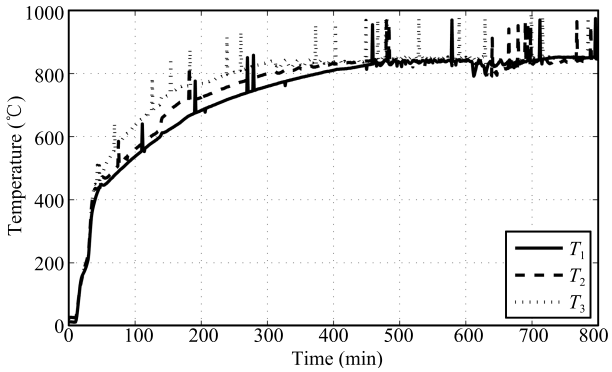

Fig. 9. Step response of three heating areas.

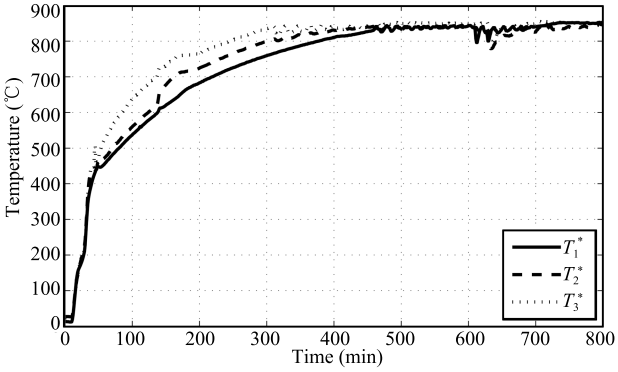

Fig. 10. Step response with median filtering.

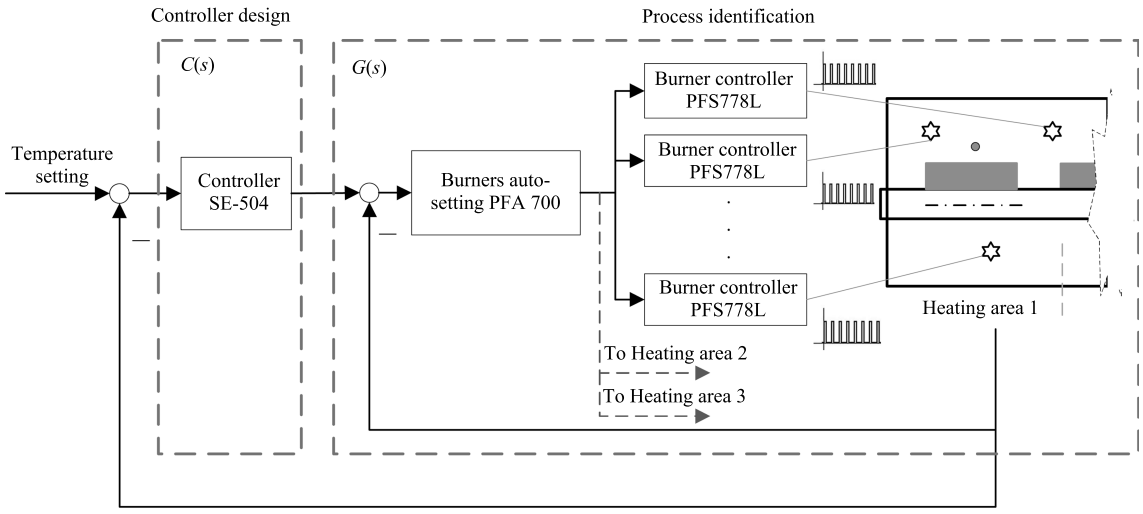

Fig. 8. Temperature control system of Titanium billet heating furnace.

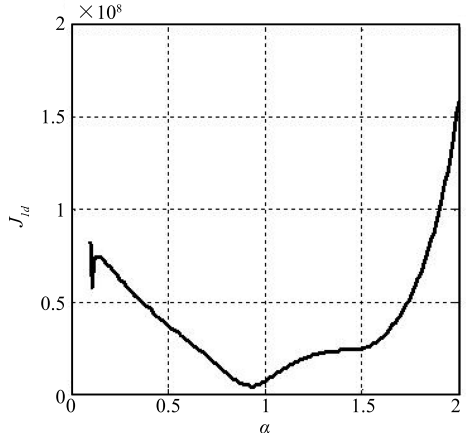

Fig. 11. Cost function for optimal identification.

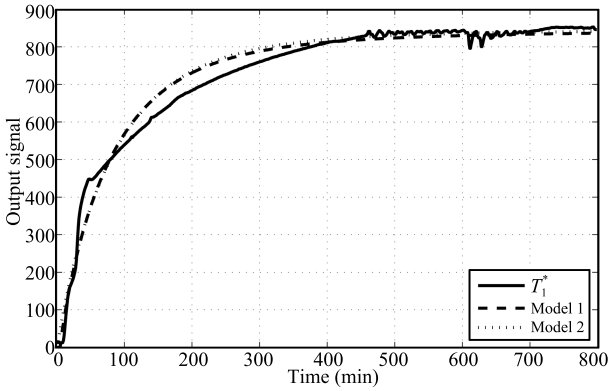

Fig. 12. Identification results for Heating area 1.

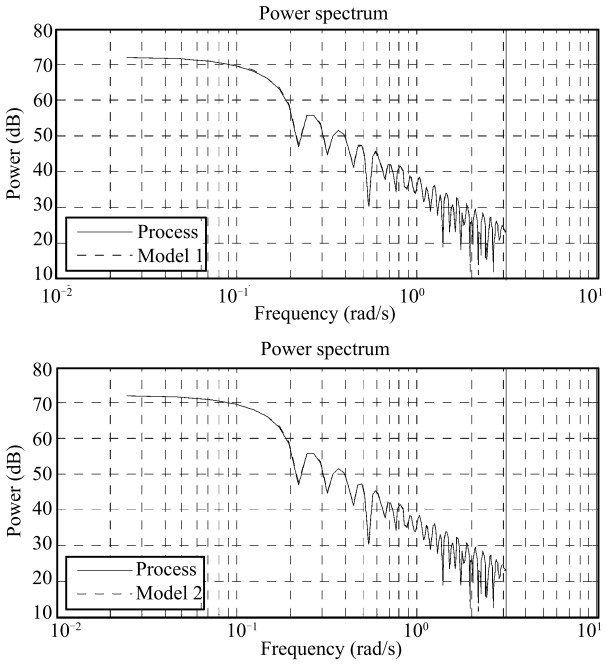

Fig. 13. Frequency spectral analysis.

frequency responses of the resultant models are nearly the same as the frequency response of the real process at low frequencies, which meets the requirement for the process with large inertia time constant. The identification results for the other two heating areas are given in Table VII and the responses are shown in Figs. 14 and 15.

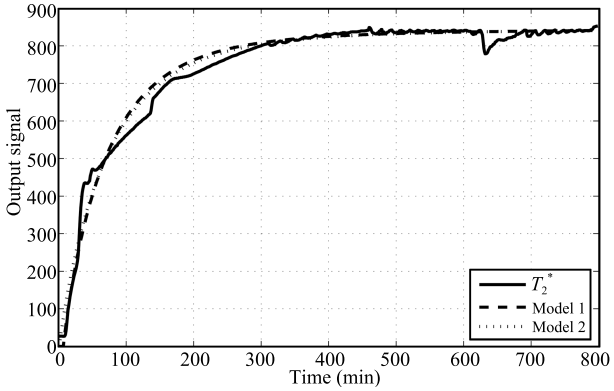

Fig. 14. Identification results for Heating area 2.

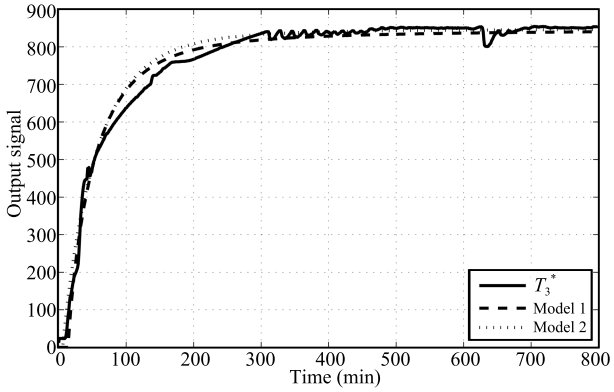

Fig. 15. Identification results for Heating area 3.

Then, we consider the temperature control for each heating area. In this case, we only provide the simulation results to show the control performance. In the simulation, three heating areas are controlled independently, and each controller is designed based on the process Model 2 in Table VII. To avoid overshoot, set $M_T = 1$, and the controller parameters are given in Table VIII. ITAE indexes are obtained in the step input response, and the achieved gain and phase margins of the resultant systems are also exhibited.

A typical heating routine requires the furnace temperature to reach 900 °C in three hours. Rather than the typical step input, ramp signal would be more practical in the heating process. According to the heating mechanism, we formulate the reference heating curve by four stages:

$$r_2(t) = \begin{cases} 10t, \\ 600, \\ 3.75(t-90)+600, \\ 900. \end{cases} \tag{50}$$

The responses, tracking errors and control inputs of three heating areas are shown in Figs. 16-18. In the first heating stage, the control inputs are increasing greatly because of the ramp input with a big slope. As we know, the steady output error is inevitable for the ramp input under PID control. The temperature tracking errors are almost kept about 100 °C in three areas. After an hour, the input signals maintain 600 °C in the second stage for the thermal insulation, and the control inputs decrease when the tracking errors become small. In the

TABLE VII
IDENTIFICATION RESULTS FOR THREE HEATING AREAS AND COMPARISONS

Process	Fractional-order model			
	Proposed (Model 1)	$J_{id} \times 10^6$	Proposed (Model 2)	$J_{id} \times 10^6$
Heating area 1	$\frac{1}{55.078s^{0.909}+1}e^{-4.91s}$	4.8788	$\frac{1}{67.1867s^{0.94}+1}e^{-5.21s}$	4.4843
Heating area 2	$\frac{1}{50.006s^{0.922}+1}e^{-6.91s}$	3.3877	$\frac{1}{56.7735s^{0.93}+1}e^{-5.92s}$	3.1368
Heating area 3	$\frac{1}{27.593s^{0.879}+1}e^{-13.49s}$	4.2200	$\frac{1}{42.817s^{0.95}+1}e^{-5.9596s}$	3.1494

TABLE VIII
PID CONTROLLERS FOR EACH HEATING AREA

Process model	k_p	k_i	k_d	ITAE	Gain margin	Phase margin
$\frac{1}{67.1867s^{0.94}+1}e^{-5.21s}$	8.2019	0.1153	0.8750	77.2937	2.871	63.8848
$\frac{1}{56.7735s^{0.93}+1}e^{-5.92s}$	7.1244	0.1090	3.9377	87.3280	2.7074	63.6843
$\frac{1}{42.817s^{0.95}+1}e^{-5.9596s}$	5.2301	0.1006	5.8289	81.9108	2.8153	65.6896

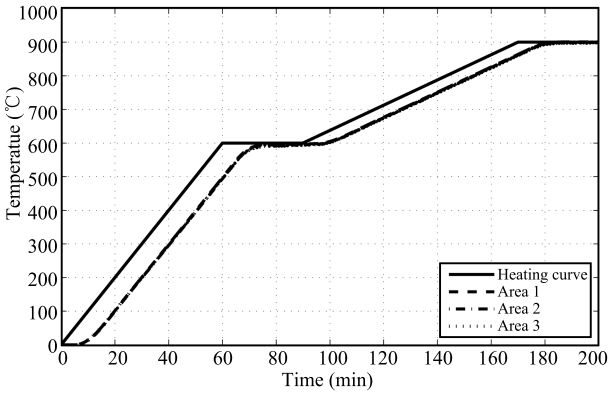

Fig. 16. Responses of three heating areas under PID control.

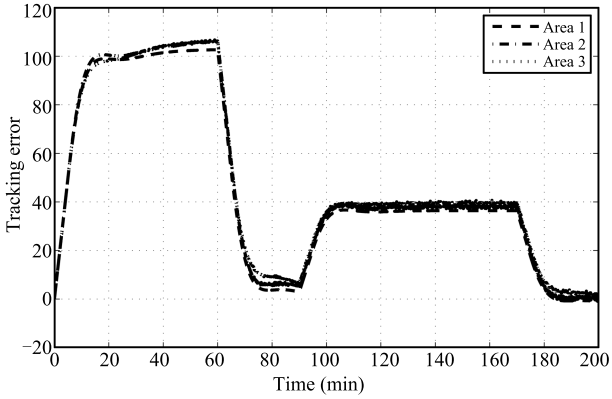

Fig. 17. Tracking Errors.

third heating stage, the control inputs increase continues with the ramp reference inputs, and the tracking errors are about 40 °C. Finally, reference inputs are kept 900 °C for half an hour in the last stage and the control inputs decrease and tend to a constant. After the temperature field distributed uniformly, all the temperature in three areas achieve 900 °C. One can see that, the proposed three PID controllers provide good control performance for the heating furnace without any overshoot and oscillation, in the whole heating process.

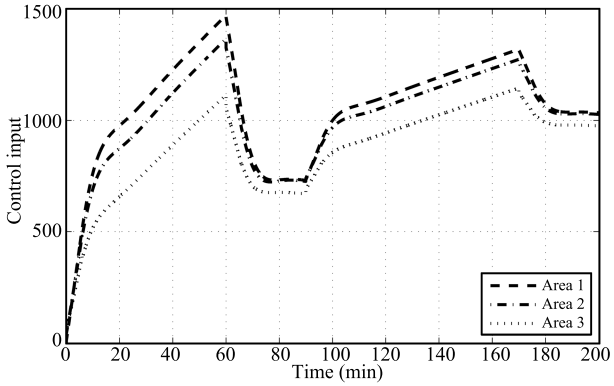

Fig. 18. Control inputs.

V. Conclusion

This paper has presented a new model identification method for a class of delay fractional-order system based on the process step response. In this method, the features of the normalized fractional-order model were analyzed and formulated by four defined characteristic functions based on the step responses. Two identification schemes were proposed based on time scaling analysis. Scheme one utilized three exact points on the step response of the process to calculate model parameters directly, and the other scheme employed optimal searching method to adjust the fractional order for the best model parameters. Simulation results show that the proposed two identification schemes were both applicable to any stable complex process, such as higher-order, under-damped/over-damped, and minimum-phase/nonminimum-phase processes.

To design a PID controller, an optimal tuning method was proposed for the delay fractional-order model. The requirements on the stability margins and negative feedback were formulated by RPC and IPC, which were implemented by trigonometric inequalities on the phase variable. With the basic variables (ϕ, ω_g, γ), an explicit PID was derived without any tedious computation, as well as the achieving of gain margins. Under the constraints of PRC and IPC, an optimal controller was obtained by the minimization of ITAE index.

Finally, the proposed method is applied to the Titanium billet heating process. Step responses of the real process were obtained and used to identify fractional-order models for three heating areas. Regarding the identified model, optimal PID controller was designed for each heating area. The application results illustrated the effectiveness of the proposed method.

REFERENCES

[1] Zhao C N, Xue D Y, Chen Y Q. A fractional order PID tuning algorithm for a class of fractional order plants. In: Proceedings of the 2005 IEEE International Conference Mechatronics and Automation. Canada: IEEE, 2005. 216−221

[2] Manabe S. A suggestion of fractional-order controller for flexible spacecraft attitude control. *Nonlinear Dynamics*, 2002, **29**(1−4): 251−268

[3] Torvik P J, Bagley R L. On the appearance of the fractional derivative in the behavior of real materials. *Journal of Applied Mechanics*, 1984, **51**(2): 294−298

[4] Nakagawa M, Sorimachi K. Basic characteristics of a fractance device. *IEICE Transactions on Fundamentals of Electronics, Communications and Computer Sciences*, 1992, **E75-A**(12): 1814−1819

[5] Özbay H, Bonnet C, Fioravanti A R. PID controller design for fractional-order systems with time delays. *Systems and Control Letters*, 2012, **61**(1): 18−23

[6] Caponetto R, Dongola G, Pappalardo F L, Tomasello V. Autotuning method for PIλDμ controllers design. *International Journal of Innovative Computing, Information and Control*, 2013, **9**(10): 4043−4055

[7] Caponetto R, Dongola G, Pappalardo F, Tomasello V. Auto-tuning and fractional order controller implementation on hardware in the loop system. *Journal of Optimization Theory and Applications*, 2013, **156**(1): 141−152

[8] Monje C A, Vinagre B M, Feliu V, Chen Y Q. Tuning and auto-tuning of fractional order controllers for industry applications. *Control Engineering Practice*, 2008, **16**(7): 798−812

[9] Monje C A, Chen Y Q, Vinagre B M, Xue D Y, Feliu-Batlle V. *Fractional-Order Systems and Controls: Fundamentals and Applications*. London: Springer-Verlag, 2010.

[10] Tavazoei M S. Time response analysis of fractional-order control systems: a survey on recent results. *Fractional Calculus and Applied Analysis*, 2014, **17**(2): 440−461

[11] Luo Y, Zhang T, Lee B, Kang C, Chen Y Q. Fractional-order proportional derivative controller synthesis and implementation for hard-disk-drive servo system. *IEEE Transactions on Control Systems Technology*, 2014, **22**(1): 281−289

[12] Oustaloup A, Sabatier J, Lanusse P, Malti R, Melchior P, Moreau X, Moze M. An overview of the crone approach in system analysis, modeling and identification, observation and control. In: Proceedings of the 17th IFAC World Congress. COEX, Korea, South: IFAC, 2008. 14254−14265

[13] Mathieu B, Le Lay L, Oustaloup A. Identification of non integer order systems in the time-domain. In: CESA'96 IMACS Multiconference: Computational Engineering in Systems Applications. 1996. 843−847

[14] Trigeassou J C, Poinot T, Lin J, Oustaloup A, Levron F. Modeling and identification of a non integer order system. In: Proceedings of the 1999 European Control Conference (ECC). Karlsruhe: IEEE, 1999. 2453−2458

[15] Poinot T, Trigeassou J C. Identification of fractional systems using an output-error technique. *Nonlinear Dynamics*, 2004, **38**(1−4): 133−154

[16] Guevara E, Meneses H, Arrieta O, Vilanova R, Visioli A, Padula F. Fractional order model identification: computational optimization. In: Proceedings of the 20th IEEE Conference on Emerging Technologies and Factory Automation (ETFA). Luxembourg: IEEE, 2015. 1−4

[17] Hartley T T, Lorenzo C F. Fractional-order system identification based on continuous order-distributions. *Signal Processing*, 2003, **83**(11): 2287−2300

[18] Jin C Y, Ryu K H, Sung S W, Lee J, Lee I B. PID auto-tuning using new model reduction method and explicit PID tuning rule for a fractional order plus time delay model. *Journal of Process Control*, 2014, **24**(1): 113−128

[19] Narang A, Shah S L, Chen T. Continuous-time model identification of fractional-order models with time delays. *IET Control Theory and Applications*, 2011, **5**(7): 900−912

[20] Luo Y, Chen Y Q, Wang C Y, Pi Y G. Tuning fractional order proportional integral controllers for fractional order systems. *Journal of Process Control*, 2010, **20**(7): 823−831

[21] Wang Y G, Shao H H. PID autotuner based on gain- and phase-margin specifications. *Industrial and Engineering Chemistry Research*, 1999, **38**(8): 3007−3012

[22] Ho W K, Lee T H, Gan O P. Tuning of multiloop proportional-integral-derivative controllers based on gain and phase margin specifications. *Industrial and Engineering Chemistry Research*, 1997, **36**(6): 2231−2238

[23] Li K Y. PID tuning for optimal closed-loop performance with specified gain and phase margins. *IEEE Transactions on Control Systems Technology*, 2013, **21**(3): 1024−1030

[24] Fung H W, Wang Q G, Lee T H. PI tuning in terms of gain and phase margins. *Automatica*, 1998, **34**(9): 1145−1149

[25] Li M D, Li D H, Wang J, Zhao C Z. Active disturbance rejection control for fractional-order system. *ISA Transactions*, 2013, **52**(3): 365−374

[26] Lv Y, Wu M, Lei Q, Nie Z Y. Soft sensor based on a Pso-Bp neural network for a titanium billet furnace-temperature. *Intelligent Automation and Soft Computing*, 2011, **17**(8): 1207−1216

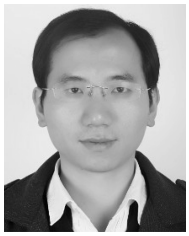

Zhuoyun Nie received the Ph. D. degree in control theory and control engineering from Central South University, China in 2012. He was a visiting scholar at the National University of Singapore. He is currently a lecturer at the School of Information Engineering, Huaqiao University, China. His research interests include robust control, process identification, internet of things, and financial forecasting. Corresponding author of this paper.

Qingguo Wang received the B. Eng. degree in chemical engineering in 1982, M. Eng. degree in 1984 and Ph. D. degree in 1987 both in industrial automation, all from Zhejiang University, China, respectively. He held Alexander-von-Humboldt Research Fellowship of Germany from 1990 to 1992. From 1992 to 2015, he was with the Department of Electrical and Computer Engineering of the National University of Singapore, where he became a full professor in 2004. He has published over 250 international journal papers and 6 books. He received nearly 1 1000 citations with h-index of 58. He is currently a distinguished professor with the Institute for Intelligent Systems, University of Johannesburg, South Africa. His present research interests include modeling, estimation, prediction, control, optimization and automation for complex systems, including but not limited to, industrial and environmental processes, new energy devices, defense systems, medical engineering, and financial markets.

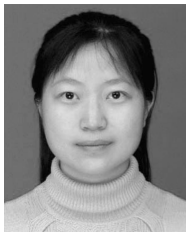

Ruijuan Liu received the Ph. D. degree in control theory and control engineering from Central South University, China in 2014. She was a visiting scholar at the University of South Wales. She is currently a lecturer at the School of Applied Mathematics, Xiamen University of Technology, China. Her research interests include robust control, nonlinear control, and disturbance rejection.

Yonghong Lan received the B. S. and M. S. degrees in applied mathematics from Xiangtan University, Xiangtan, China in 1999 and 2004, respectively; and the Ph. D. degree in control theory and control engineering from Central South University, Changsha, China in 2010. He is currently an assistant professor at the School of Information Engineering, Xiangtan University, Xiangtan, China. His current research interests include fractional order control systems.